

# Probing parton saturation and the gluon dipole via diffractive jet production at the Electron-Ion Collider

E. Iancu,<sup>1,\*</sup> A.H. Mueller,<sup>2,†</sup> and D.N. Triantafyllopoulos<sup>3,‡</sup>

<sup>1</sup>*Université Paris-Saclay, CNRS, CEA, Institut de physique théorique, F-91191, Gif-sur-Yvette, France*

<sup>2</sup>*Department of Physics, Columbia University, New York, NY 10027, USA*

<sup>3</sup>*European Centre for Theoretical Studies in Nuclear Physics and Related Areas (ECT\*) and Fondazione Bruno Kessler, Strada delle Tabarelle 286, I-38123 Villazzano (TN), Italy*

(Dated: April 26, 2022)

We demonstrate that hard dijet production via coherent inelastic diffraction is a promising channel for probing gluon saturation at the Electron-Ion Collider. By *inelastic* diffraction we mean a process in which the two hard jets — a quark-antiquark pair generated by the decay of the virtual photon — are accompanied by a softer gluon jet, emitted by the quark or the antiquark. This process can be described as the elastic scattering of an effective gluon-gluon dipole. The cross section takes a factorised form, between a hard factor and a unintegrated (“Pomeron”) gluon distribution describing the transverse momentum imbalance between the hard dijets. The dominant contribution comes from the black disk limit and leads to a dijet imbalance of the order of the target saturation momentum  $Q_s$  evaluated at the rapidity gap. Integrating out the dijet imbalance, we obtain a collinear factorization where the initial condition for the DGLAP evolution is set by gluon saturation.

*Introduction.* A class of observables that attracted much attention over the last years refers to the production of a pair of jets in “dilute-dense” collisions (electron-nucleus, proton-nucleus, ultraperipheral proton-nucleus and nucleus-nucleus) at high energy [1–28]. Through the correlations among the produced jets, these observables have the potential to probe fine aspects of the gluon distribution in the dense target, like the onset of saturation [29–31], or the spatial distribution in the plane transverse to the collision axis [10, 11]. It was furthermore observed that the physical content of such observables becomes more transparent in the “correlation limit” where the two measured jets are relatively hard and propagate nearly back-to-back in the transverse plane [3–5, 12–15, 17, 18]. This means that their individual transverse momenta  $k_{1\perp} = |\mathbf{k}_1|$  and  $k_{2\perp} = |\mathbf{k}_2|$  are much larger than their transverse imbalance:  $k_{1\perp} \simeq k_{2\perp} \gg K_{\perp} \equiv |\mathbf{k}_1 + \mathbf{k}_2|$ . This limit often permits to factorise the interesting correlations (which refer to the distribution w.r.t.  $\mathbf{K}$ ) from the comparatively hard physics of dijet production.

Specialising to the case of electron-nucleus deep inelastic scattering (DIS) at high energies, one particular example that serves as a benchmark for our new results, is the inclusive dijet production. In the correlation limit, the respective cross-section (as computed in the CGC formalism [29–31]) takes a factorised form, recognised as the high-energy limit of the TMD factorisation [3]: it is the product between a *hard factor* describing the photon dissociation into a quark-antiquark ( $q\bar{q}$ ) pair (a “colour dipole”) together with the coupling between this pair and the target gluons, and a *unintegrated gluon distribution* (UGD), the “Weizsäcker-Williams gluon TMD”, describing the transverse momentum transfer from the target to the  $q\bar{q}$  dijet, via inelastic collisions.

In the presence of gluon saturation, the typical transferred momentum cannot be smaller than the target satu-

ration momentum  $Q_s(Y)$  at the rapidity scale  $Y$  probed by the scattering. The correlation limit applies when  $k_{1\perp}, k_{2\perp} \gg Q_s(Y)$ . This in turn requires a relatively hard DIS process, with  $Q^2 \gg Q_s^2(Y)$ . However, very large values of  $Q^2$  lead to an enhanced radiation in the final state, which may obscure the physics of saturation, due to the Sudakov effect [32]: the recoil associated with these emissions can dominate the dijet momentum imbalance, to the detriment of gluon saturation [9].

*Diffractive trijet production in the correlation limit.* In this Letter, we propose another hard dijet process in DIS at high energy, which is even more sensitive to gluon saturation than the inclusive dijet production. This is the production of a pair of hard jets in the correlation limit, via coherent inelastic diffraction.

“Diffraction” refers to a process in which there is a large rapidity gap between the produced jets and the nuclear target, while “inelastic” means that the two hard jets — the  $q\bar{q}$  pair generated by the decay of the virtual photon — are accompanied by a softer gluon ( $g$ ) jet, with transverse momentum  $\mathbf{k}_3$ , emitted by the quark or the antiquark. “Coherent” means that the hadronic target (proton or nucleus) does not break in the final state, so the rapidity gap (denoted as  $Y_{\mathbb{P}}$ ) lies on the target side.

In such a coherent process, the scattering between the  $q\bar{q}g$  system and the hadronic target is necessarily elastic. This implies that the transverse momentum transferred by the target is quite small,  $\Delta_{\perp} \sim 2/R \sim \Lambda$  ( $R$  is the target radius and  $\Lambda$  the QCD confinement scale). This is negligible compared to the recoil associated with the gluon emission, which therefore controls the transverse momentum imbalance  $\mathbf{K} = \mathbf{k}_1 + \mathbf{k}_2$  between the two hard jets:  $\mathbf{K} \simeq -\mathbf{k}_3$ . The “correlation limit” of interest corresponds to  $k_{1\perp} \simeq k_{2\perp} \gg k_{3\perp}$ . This is in fact the *typical* trijet configuration for sufficiently hard diffraction,  $Q^2 \gg Q_s^2(Y_{\mathbb{P}})$ , as we now explain.

The quark and the antiquark produced by the decay of a hard virtual photon have transverse momenta of the order of the virtuality,  $k_{1\perp}, k_{2\perp} \sim Q$ , whereas the momentum  $k_{3\perp}$  of the gluon jet is controlled by the scattering and is typically of order  $Q_s(Y_{\mathbb{P}})$ . The last point is specific to diffraction: the elastic cross-section involves the *square* of the forward scattering amplitude, hence it is more sensitive than the total cross-section to the “black disk limit” where the scattering is strong and  $k_{3\perp} \sim Q_s(Y_{\mathbb{P}})$ .

In practice, we propose the experimental measurement of the hard dijets *alone*. But albeit not directly measured, the comparatively soft, gluon, jet has a crucial influence on the structure of the final state: (i) it controls the momentum imbalance between the two hard jets, and (ii) it opens up the colour space and thus yields a large size partonic configuration to probe gluon saturation in the target.

Diffraction trijet production has also been addressed in the context of  $k_T$ -factorisation, more than 2 decades ago [33]. However that early study has overlooked the key role of gluon saturation. The effects of saturation have been included (within the dipole picture) in [34], but the focus there was on diffractive gluon production only.

*The kinematics for trijet diffractive production.* We describe DIS within the dipole picture, applicable at small Bjorken  $x_{\text{Bj}} \equiv Q^2/(2q \cdot P_N) \ll 1$ , with  $q^\mu$  and  $P_N^\mu$  the 4-momenta of the virtual photon and, respectively, of a nucleon from the target (assumed to be massless). We work in a frame where  $q^\mu = (q^+, -Q^2/2q^+, \mathbf{0})$  and  $P_N^\mu = (0, P_N^-, \mathbf{0})$ , in light-cone notations.

We denote the 4-momenta of the produced partons as  $k_i^\mu = (k_i^+, k_i^-, \mathbf{k}_i)$ , with  $k_i^- = k_{i\perp}^2/2k_i^+$ , where  $i = 1, 2, 3$  refers to the quark, the antiquark, and the gluon, respectively. We shall mostly work with the longitudinal fractions  $\vartheta_i = k_i^+/q^+$ , with  $\vartheta_1 + \vartheta_2 + \vartheta_3 = 1$ , and we shall denote  $\xi \equiv \vartheta_3$  for the gluon. We anticipate that the interesting situation is such that  $\xi \ll 1$ , whereas  $\vartheta_1$  and  $\vartheta_2$  are comparable with each other.

For the  $q\bar{q}$  pair, we replace  $\mathbf{k}_1$  and  $\mathbf{k}_2$  with  $\mathbf{P}$  and  $\mathbf{K}$ , where  $\mathbf{P} = \vartheta_2\mathbf{k}_1 - \vartheta_1\mathbf{k}_2$  is the relative momentum and  $\mathbf{K} = \mathbf{k}_1 + \mathbf{k}_2$  is the total momentum. We neglect the transverse momentum transfer from the target,  $\mathbf{k}_1 + \mathbf{k}_2 + \mathbf{k}_3 = \mathbf{0}$ , and focus on the correlation limit for the hard dijets:  $P_\perp \sim Q \gg K_\perp = k_{3\perp} \sim Q_s(Y_{\mathbb{P}})$ .

The elastic amplitude will be first constructed in transverse coordinate space, to take profit of the eikonal approximation. We denote the transverse coordinates of the 3 partons as  $\mathbf{x}$ ,  $\mathbf{y}$  and  $\mathbf{z}$  (see Fig. 1). For the  $q\bar{q}$  pair, we shall also use  $\mathbf{r} = \mathbf{x} - \mathbf{y}$  (the transverse separation) and  $\mathbf{b} = \vartheta_1\mathbf{x} + \vartheta_2\mathbf{y}$  (the centre-of-energy).

To characterise the rapidity distribution of the final state, we use the standard variables for diffraction,

$$\beta \equiv \frac{Q^2}{Q^2 + M_{q\bar{q}}^2}, \quad x_{\mathbb{P}} \equiv \frac{Q^2 + M_{q\bar{q}}^2}{2q \cdot P_N}, \quad (1)$$

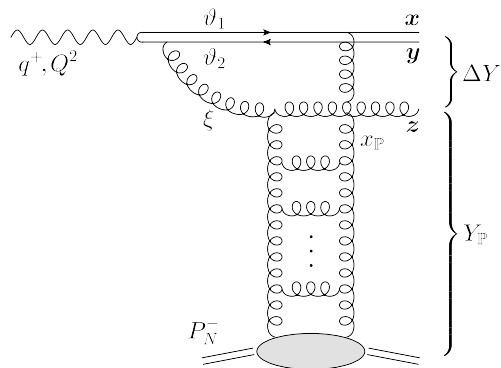


FIG. 1. Schematic representation of a Feynman graph contributing to diffractive trijet production. The colourless, “Pomeron”, exchange is represented by the gluon ladder.

with the diffractive mass  $M_{q\bar{q}}^2 \equiv (k_1 + k_2 + k_3)^2$ , or

$$M_{q\bar{q}}^2 = \frac{k_{1\perp}^2}{\vartheta_1} + \frac{k_{2\perp}^2}{\vartheta_2} + \frac{k_{3\perp}^2}{\vartheta_3} = M_{q\bar{q}}^2 + K_\perp^2 + \frac{k_{3\perp}^2}{\xi}, \quad (2)$$

where  $M_{q\bar{q}}^2 \equiv (k_1 + k_2)^2 = P_\perp^2/(\vartheta_1\vartheta_2)$ . Notice that  $\beta x_{\mathbb{P}} = x_{\text{Bj}}$ , or  $Y = \Delta Y + Y_{\mathbb{P}}$ , where  $Y = \ln(1/x_{\text{Bj}})$  is the rapidity difference between the target and the virtual photon,  $\Delta Y = \ln(1/\beta)$  is the rapidity phase-space occupied by the  $q\bar{q}g$  system, and  $Y_{\mathbb{P}} = \ln(1/x_{\mathbb{P}})$  is the rapidity gap between this system and the target.

*The gluon dipole picture.* The aforementioned hierarchy of transverse scales implies an appealing physical picture. The hard scale  $P_\perp$  controls the size  $\mathbf{r} = \mathbf{x} - \mathbf{y}$  of the  $q\bar{q}$  pair,  $r \sim 1/P_\perp$ , whereas the gluon transverse momentum  $k_{3\perp}$  controls the transverse separation  $\mathbf{R} = \mathbf{z} - \mathbf{b}$  between the gluon and its sources:  $R \sim 1/k_{3\perp}$ . So, when  $k_{3\perp} \ll P_\perp$ , we also have  $R \gg r$ , and the  $q\bar{q}g$  projectile effectively scatters as a *gluon-gluon (gg) dipole*. One leg of this dipole is the emitted gluon and the other leg is made with the  $q\bar{q}$  pair, which remains in a colour octet state after the gluon emission. A similar picture has been used for computing the  $q\bar{q}g$  contribution to the diffractive structure function [35, 36].

The validity of this picture also depends upon the longitudinal scales in the problem. For the typical events, the gluon formation time  $\tau_3 = 2k_3^+/k_{3\perp}^2$  with  $k_3^+ = \xi q^+$  should not exceed the coherence time  $\tau_q = 2q^+/Q^2$  of the virtual photon. This implies  $\xi \lesssim k_{3\perp}^2/Q^2$ .

In the correlation limit  $k_{3\perp} \sim Q_s \ll Q$ , the gluon is *soft*,  $\xi \lesssim Q_s^2/Q^2 \ll 1$ , which greatly simplifies the evaluation of its emission vertex. However,  $\xi$  should not be *too* small either, since we would like to avoid the emission of additional soft gluons, which would modify the colour flow and thus spoil the gluon dipole picture. The phase-space for soft gluon emissions by the  $q\bar{q}$  pair is  $\Delta Y = \ln(1/\beta)$  and we shall require  $\alpha_s \Delta Y \ll 1$ . Using  $M_{q\bar{q}}^2 \sim Q_s^2/\xi$  for very small  $\xi$ , cf. Eq. (2), we conclude that our picture applies to  $\xi$  values obeying  $e^{-1/\alpha_s} \ll \xi Q^2/Q_s^2 \lesssim 1$ . This is a parametrically wide range when the coupling is weak.

The most interesting region for studying saturation is the upper end of this window at  $\xi \sim Q_s^2/Q^2$ , since then  $\Delta Y \lesssim 1$  and the rapidity gap is as large as possible:  $Y \simeq Y_{\mathbb{P}}$ . Hence most of the total rapidity  $Y$  is used for the high-energy evolution of the ‘‘Pomeron’’ — the colourless exchange between the jets and the target, as materialised by the gluon dipole scattering amplitude. In practice, we shall mostly work with smaller values  $\xi \ll Q_s^2/Q^2$ , since this allows for an important simplification: the gluon emission can be computed in the eikonal approximation and then it factorises. The generalisation to larger values  $\xi \sim Q_s^2/Q^2$  will be briefly discussed towards the end and further detailed in a subsequent publication [37].

These kinematical constraints are (at least marginally)

$$\frac{d\sigma_D^{\gamma_T^* A \rightarrow q\bar{q}gA'X}}{d\vartheta_1 d\vartheta_2 d\xi d^2\mathbf{P} d^2\mathbf{K} d^2\mathbf{k}_3} = S_\perp \frac{\alpha_{em} N_c}{2\pi^4} \left( \sum e_f^2 \right) (\vartheta_1^2 + \vartheta_2^2) \delta(1 - \vartheta_1 - \vartheta_2) \delta^{(2)}(\mathbf{K} + \mathbf{k}_3) \frac{\alpha_s C_F}{\xi} \sum_{lj} |\mathcal{A}_{q\bar{q}g}^{lj}|^2, \quad (3)$$

where the elastic amplitude takes a factorised form,

$$\mathcal{A}_{q\bar{q}g}^{lj} = \mathcal{H}^{li}(\mathbf{P}, \bar{Q}) \mathcal{G}^{ij}(\mathbf{K}, Y_{\mathbb{P}}). \quad (4)$$

The hard factor (with  $\int_{\mathbf{r}} = \int d^2\mathbf{r}$  and  $\bar{Q}^2 \equiv \vartheta_1 \vartheta_2 Q^2$ )

$$\mathcal{H}^{li}(\mathbf{P}, \bar{Q}) = \frac{1}{2\pi} \int_{\mathbf{r}} e^{-i\mathbf{P}\cdot\mathbf{r}} \frac{r^l r^i}{r} \bar{Q} K_1(\bar{Q}r), \quad (5)$$

describes the decay  $\gamma_T^* \rightarrow q\bar{q}$  of the virtual photon and the vertex  $\propto r^i$  for the emission of a transverse gluon from the small  $q\bar{q}$  dipole. The tensorial distribution

$$\begin{aligned} \mathcal{G}^{ij}(\mathbf{K}, Y) &\equiv \int_{\mathbf{R}} e^{i\mathbf{K}\cdot\mathbf{R}} \left( \delta^{ij} - \frac{2R^i R^j}{R^2} \right) \frac{\mathcal{T}_g(R, Y)}{2\pi R^2} \\ &= \left( \frac{K_\perp^i K_\perp^j}{K_\perp^2} - \frac{\delta^{ij}}{2} \right) \mathcal{G}(K_\perp, Y), \end{aligned} \quad (6)$$

encodes the spatial distribution of the gluon emission by the small  $q\bar{q}$  pair (a dipolar colour field) together with the scattering between the effective  $g\bar{g}$  dipole and the target. The scattering amplitude  $\mathcal{T}_g(R, Y)$  is defined as (we recall that  $\mathbf{R} = \mathbf{z} - \mathbf{b}$ )

$$\mathcal{T}_g(R, Y) = 1 - \frac{1}{N_c^2 - 1} \left\langle \text{tr}(U_{\mathbf{z}} U_{\mathbf{b}}^\dagger) \right\rangle_Y, \quad (7)$$

where  $U_{\mathbf{z}}, U_{\mathbf{b}}^\dagger$  are Wilson lines in the adjoint representation and the brackets denote the CGC average over the colour fields in the target [29, 30]. The CGC weight function includes the high-energy, BK/JIMWLK, evolution [41–48], up to the rapidity scale  $Y$ .

consistent with the range that should be covered by the EIC [38, 39]; e.g. for  $x_{\text{Bj}} = 10^{-3}$ , one will be able to measure DIS processes with  $Q^2 \leq 10 \text{ GeV}^2$ , whereas the nuclear (Pb) saturation momentum is estimated as  $Q_s^2 \simeq 1.5 \text{ GeV}^2$ . Clearly, the situation would be even more favorable (higher energies, smaller  $x_{\text{Bj}}$ , and larger  $Q^2$ ) at the Large Hadron-Electron Collider [40].

*The diffractive trijet cross-section.* When the gluon is sufficiently soft ( $k_{3\perp} \ll P_\perp \sim Q$  and  $\xi \ll k_{3\perp}^2/Q^2$ ), its emission can be computed in the eikonal approximation. For a virtual photon with transverse polarisation<sup>1</sup>, a homogeneous target with transverse area  $S_\perp$ , and three flavours of massless quarks,  $f = u, d, s$ , the trijet cross-section reads (with  $\alpha_{em} = e^2/4\pi$ ) [37]

Using the second line of Eq. (6), one finds  $\sum_{lj} |\mathcal{A}_{q\bar{q}g}^{lj}|^2 = \frac{1}{4} \sum_{li} |\mathcal{H}^{li}|^2 \mathcal{G}^2$  with

$$\sum_{li} |\mathcal{H}^{li}|^2(\mathbf{P}, \bar{Q}) = 2 \frac{P_\perp^4 + \bar{Q}^4}{(P_\perp^2 + \bar{Q}^2)^4}. \quad (8)$$

*The hard dijet cross-section.* The cross-section for the diffractive production of the  $q\bar{q}$  dijets is obtained from (3) by integrating out the kinematical variables  $\mathbf{k}_3$  and  $\xi$  of the unmeasured gluon jet. The integral over  $\mathbf{k}_3$  is trivial and yields  $k_{3\perp} = K_\perp$ . The value of  $\xi$  is in fact fixed by the rapidity gap: Eqs. (1)–(2) imply

$$\frac{d\xi}{\xi} = \frac{dx_{\mathbb{P}}}{x_{\mathbb{P}} - x_{q\bar{q}}} \quad \text{with} \quad x_{q\bar{q}} \equiv \frac{Q^2 + M_{q\bar{q}}^2 + K_\perp^2}{2P_N \cdot q}. \quad (9)$$

When  $\xi \ll K_\perp^2/Q^2$ , the diffractive mass (2) is dominated by the soft gluon,  $M_{q\bar{q}}^2 \simeq K_\perp^2/\xi \gg M_{q\bar{q}}^2 \sim Q^2$ , hence  $x_{q\bar{q}} \ll x_{\mathbb{P}}$  and  $d\xi/\xi \simeq dx_{\mathbb{P}}/x_{\mathbb{P}} = dY_{\mathbb{P}}$ . The dijet cross-section per unit rapidity gap is then obtained as

$$\frac{d\sigma_D^{\gamma_T^* A \rightarrow q\bar{q}A'X}}{d\vartheta_1 d\vartheta_2 d^2\mathbf{P} d^2\mathbf{K} dY_{\mathbb{P}}} = H(x_{q\bar{q}}, Q^2, P_\perp^2) \frac{dx G_{\mathbb{P}}(x, x_{\mathbb{P}}, K_\perp^2)}{d^2\mathbf{K}}, \quad (10)$$

with the hard impact factor:

$$\begin{aligned} H(x_{q\bar{q}}, Q^2, P_\perp^2) &\equiv \alpha_{em} \alpha_s \left( \sum e_f^2 \right) \delta(1 - \vartheta_1 - \vartheta_2) \\ &\times (\vartheta_1^2 + \vartheta_2^2) \frac{P_\perp^4 + \bar{Q}^4}{(P_\perp^2 + \bar{Q}^2)^4}, \end{aligned} \quad (11)$$

and the unintegrated gluon distribution of the Pomeron:

$$\frac{dx G_{\mathbb{P}}(x, x_{\mathbb{P}}, K_\perp^2)}{d^2\mathbf{K}} \equiv S_\perp \frac{N_c^2 - 1}{8\pi^4} [\mathcal{G}(K_\perp, Y_{\mathbb{P}})]^2. \quad (12)$$

<sup>1</sup> The results for a longitudinal photon are readily obtained by replacing  $\vartheta_1^2 + \vartheta_2^2 \rightarrow 4\vartheta_1 \vartheta_2$  in (3) and  $P_\perp^4 + \bar{Q}^4 \rightarrow 2P_\perp^2 \bar{Q}^2$  in (8).

Here,  $x \equiv x_{q\bar{q}}/x_{\mathbb{P}} \ll 1$  is the fraction of the Pomeron longitudinal momentum transferred to the hard dijets and  $\mathcal{G}(K_{\perp}, Y_{\mathbb{P}})$  is related to the gluon dipole amplitude via

$$\mathcal{G}(K_{\perp}, Y_{\mathbb{P}}) = 2 \int_0^{\infty} \frac{dR}{R} J_2(K_{\perp}R) \mathcal{T}_g(R, Y_{\mathbb{P}}). \quad (13)$$

This Bessel transform is controlled by dipole sizes  $R \lesssim 1/K_{\perp}$ . Let us consider two interesting limits:

(i) for large momenta  $K_{\perp} \gg Q_s(Y_{\mathbb{P}})$ , we use the single scattering approximation where  $\mathcal{T}_g(R, Y_{\mathbb{P}})$  is proportional to dipole area  $R^2$  and to the target gluon distribution per unit transverse area; this gives

$$\mathcal{G}(K_{\perp}, Y_{\mathbb{P}}) \simeq \frac{4\pi^2 N_c}{N_c^2 - 1} \frac{\alpha_s}{K_{\perp}^2} \left. \frac{dxG(x, K_{\perp}^2)}{d^2\mathbf{b}} \right|_{x=x_{\mathbb{P}}}. \quad (14)$$

(ii) for lower momenta  $K_{\perp} \ll Q_s(Y_{\mathbb{P}})$ , we use the black disk limit  $\mathcal{T}_g = 1$  to find

$$\mathcal{G}(K_{\perp}, Y_{\mathbb{P}}) \simeq 1. \quad (15)$$

In the McLerran-Venugopalan (MV) model [49, 50], one can quasi-exactly compute the integral in Eq. (13) and thus find a global approximation interpolating between the two above limits:

$$\mathcal{G}(K_{\perp}) = \frac{Q_A^2}{K_{\perp}^2} \ln \frac{K_{\perp}^2}{\Lambda^2} \left[ 1 - \exp \left\{ - \frac{K_{\perp}^2}{Q_A^2 \ln(K_{\perp}^2/\Lambda^2)} \right\} \right]. \quad (16)$$

The scale  $Q_A^2 \propto A^{1/3}$  is related to the saturation momentum of the MV model via  $Q_s^2 = Q_A^2 \ln(Q_s^2/\Lambda^2)$  [29].

To summarise, the distribution  $[\mathcal{G}(K_{\perp})]^2$  which enters the dijet cross-section (10) is of order one when  $K_{\perp} \lesssim Q_s$ , but is rapidly decreasing, as  $1/K_{\perp}^4$ , when  $K_{\perp} \gg Q_s$ . This means that the typical value of the dijet momentum imbalance is  $K_{\perp} \sim Q_s(Y_{\mathbb{P}})$ , as anticipated. So, albeit relatively hard ( $P_{\perp}^2 \sim Q^2 \gg Q_s^2$ ), this diffractive process is strongly sensitive to gluon saturation.

This sensitivity is stronger than for *inclusive* dijets in the correlation limit: in that case too, the saturation effects are important when  $K_{\perp} \lesssim Q_s$ . However, at larger momenta  $K_{\perp} \gg Q_s$ , the cross-section decays only as  $1/K_{\perp}^2$ . Hence most of the inclusive dijet events lie in the tail of the distribution at large momenta ( $Q_s \ll K_{\perp} \ll P_{\perp}$ ), where saturation is unimportant.

Implicit in Eqs. (10)–(12) is the shift to a new physical picture, where the gluon is emitted by the Pomeron and the small  $q\bar{q}$  dipole inelastically scatters off this gluon, thus acquiring a momentum imbalance  $\mathbf{K}$ . This picture would be manifest if the calculation was performed in the target light-cone gauge  $A^- = 0$  (see e.g. [51]), as opposed to the gauge  $A^+ = 0$  implicitly used in deriving Eq. (3). This *a posteriori* change of picture is possible due to the strong hierarchy of transverse momentum scales,  $P_{\perp}^2 \sim Q^2 \gg K_{\perp}^2 \sim Q_s^2$ , which is the premise of the collinear factorisation.

Indeed the factorised structure of the diffractive cross-section (10) is similar to the TMD factorisation for the inclusive dijet production in the correlation limit [3–5]. The hard impact factor is *exactly* the same, whereas the Weizsäcker-Williams gluon TMD is replaced by the unintegrated gluon distribution of the Pomeron, Eq. (12).

*Collinear factorisation and the gluon distribution of the Pomeron.* When  $P_{\perp} \gg K_{\perp}$ , the dijet cross-section is expected to receive radiative corrections enhanced by the Sudakov double logarithm  $\ln^2(P_{\perp}^2/K_{\perp}^2)$  [32]. Such corrections could modify the  $K_{\perp}$ -distribution of the measured dijets and thus hinder the signal of gluon saturation. To avoid this problem, we propose to integrate the cross-section over  $K_{\perp}$ , up to the hard scale  $P_{\perp}$ :

$$\frac{d\sigma_D^{\gamma_T^* A \rightarrow q\bar{q} A' X}}{d\theta_1 d\theta_2 d^2\mathbf{P} dY_{\mathbb{P}}} = H(x_{q\bar{q}}, Q^2, P_{\perp}^2) xG_{\mathbb{P}}(x, x_{\mathbb{P}}, P_{\perp}^2), \quad (17)$$

where  $x = x_{q\bar{q}}/x_{\mathbb{P}}$  and  $xG_{\mathbb{P}}(x, x_{\mathbb{P}}, P_{\perp}^2)$  is the gluon distribution of the Pomeron, as obtained by integrating Eq. (12) over  $K_{\perp}$ . Eq. (17) is recognised as the collinear factorisation for the diffractive process at hand.

Unlike for the *inclusive* dijets, where the integration over  $K_{\perp}$  has the drawback to wash out the sensitivity to gluon saturation, there is no similar difficulty for the diffractive dijets: the function  $[\mathcal{G}(K_{\perp})]^2$  is rapidly decreasing when  $K_{\perp} \gg Q_s$ , so its integral is dominated by  $K_{\perp} \sim Q_s$  and is independent of the upper cutoff  $P_{\perp}$ :

$$\int d^2\mathbf{K} [\mathcal{G}(K_{\perp})]^2 = 4 \int_{\mathbf{R}} \frac{\mathcal{T}_g^2(R)}{R^4} \simeq \pi\kappa Q_s^2(Y_{\mathbb{P}}), \quad (18)$$

with  $\kappa$  a number depending on our approximation for  $\mathcal{T}_g(R)$ ; e.g., the MV model (16) yields  $\kappa = 2 \ln 2$ . Thus, quite remarkably, the physics of saturation determines the Pomeron gluon distribution which enters the collinear factorisation at the scale  $Q^2 \gtrsim Q_s^2$ . In turn, this can be used as an initial condition for the DGLAP evolution towards larger values  $Q^2 \gg Q_s^2$ .

*Initial condition for DGLAP evolution from gluon saturation.* So far, the Pomeron UGD in Eq. (12) has been constructed for  $x \ll 1$ , but the initial condition for the DGLAP equation is needed for generic values  $x \leq 1$ . Using  $(1-x)/x \sim K_{\perp}^2/\xi Q^2$  (cf. Eqs. (1), (2) and (9)), one sees that  $x \sim \mathcal{O}(1)$  corresponds to  $\xi \gtrsim K_{\perp}^2/Q^2$ , i.e. to gluon emissions with relatively large formation times  $\tau_3 \gtrsim \tau_q$ , for which the eikonal approximation does not apply anymore. So long as we stay in the correlation limit  $Q^2 \gg K_{\perp}^2$ , one can still use the condition  $\xi \ll 1$  to simplify the gluon emission vertex. However, one now needs a more accurate treatment of the light-cone energy denominators. This will be detailed in Ref. [37], but the main results are quite simple: to parametric accuracy, it suffices to restrict the integral in Eq. (13) to dipole sizes

$$R^2 \lesssim \frac{1}{\xi Q^2} \sim \frac{1-x}{x K_{\perp}^2}. \quad (19)$$

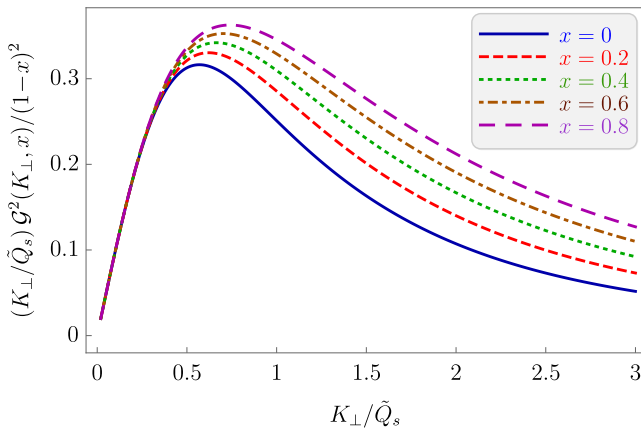


FIG. 2. The UGD of the Pomeron  $\mathcal{G}(K_\perp, x)$  obtained from an extension of Eq. (13) valid for generic values of  $x \equiv x_{q\bar{q}}/x_{\mathbb{P}}$  [37]. We use the MV model for  $\mathcal{T}_g(R)$  and plot the function  $(K_\perp/\tilde{Q}_s)[\mathcal{G}(K_\perp, x)/(1-x)]^2$ , with  $\tilde{Q}_s^2 = (1-x)Q_s^2$ , as a function of  $K_\perp/\tilde{Q}_s$ , for various values of  $x$ .

Hence, for  $x \sim \mathcal{O}(1)$ , the transverse separation  $R$  between the gluon and the  $q\bar{q}$  pair at the time of scattering is considerably smaller than its final value  $R_f \sim 1/K_\perp$  at the time of emission. This is understood as follows: in a quantum emission, the gluon separates from its sources via diffusion,  $R^2(\tau) \sim \tau/k_3^+$ , until a time  $\tau \sim \tau_3$ , when  $R(\tau_3) = R_f$  and the gluon is freed. However, when  $\tau_3$  is larger than the typical scattering time (here, of order  $\tau_q$ ), then  $R^2(\tau_q) \sim \tau_q/k_3^+ \sim 1/(\xi Q^2)$  is necessarily smaller than  $R_f^2$ , by a factor  $\tau_q/\tau_3 = (1-x)/x$ .

The main effect of this new constraint is to introduce an effective,  $x$ -dependent, saturation momentum,  $\tilde{Q}_s^2(x, Y_{\mathbb{P}}) \equiv (1-x)Q_s^2(Y_{\mathbb{P}})$ , which separates between weak and strong scattering for generic  $x$  [37]. Roughly speaking, the function  $\mathcal{G}(K_\perp, x)$  can be obtained from its value at small- $x$  by replacing  $Q_s \rightarrow \tilde{Q}_s(x)$  and multiplying the result by  $(1-x)$  (see Fig. 2). Integrating over  $K_\perp^2$  gives the following estimate for the Pomeron gluon distribution at  $Q^2 \gtrsim Q_s^2(Y_{\mathbb{P}})$  and arbitrary  $x \equiv x_{q\bar{q}}/x_{\mathbb{P}}$ :

$$xG_{\mathbb{P}}(x, x_{\mathbb{P}}, Q^2) = S_\perp (1-x)^2 \frac{N_c^2 - 1}{(2\pi)^3} \kappa Q_s^2(Y_{\mathbb{P}}). \quad (20)$$

This expression, emerging from first principles, can be used as an initial condition for the DGLAP equation.

*Summary and perspectives.* We have shown that hard diffractive production of 3 jets in the correlation limit is a sensitive probe of gluon saturation in DIS at small  $x$ . This sensitivity persists after integrating over the kinematics of the soft jet to obtain the collinear factorisation for the hard dijets. Our analysis has focused on the main phenomena. Explicit results have been presented in the MV model, for simplicity. The effects of the pQCD evolution can be numerically important and also conceptually interesting, because of the interplay between the BK/JIMWLK and the DGLAP evolutions. We will in-

clude these effects in a subsequent study [37]. It would be interesting to better understand the interplay between the Sudakov effects and gluon saturation on the dijet distribution in the momentum imbalance  $K_\perp$ . Last but not least, one may think about a similar process in ultraperipheral proton-nucleus, or nucleus-nucleus, collisions at the LHC, where the available energies are much higher.

**Acknowledgements** The work of E.I. is supported in part by the Agence Nationale de la Recherche project ANR-16-CE31-0019-01. The work of A.H.M. is supported in part by the U.S. Department of Energy Grant # DE-FG02-92ER40699.

\* edmond.iancu@ipht.fr

† ahm4@columbia.edu

‡ trianta@ectstar.eu

- [1] C. Marquet, “Forward inclusive dijet production and azimuthal correlations in pA collisions,” *Nucl. Phys.* **A796** (2007) 41–60, [arXiv:0708.0231 \[hep-ph\]](#).
- [2] J. L. Albacete and C. Marquet, “Azimuthal correlations of forward di-hadrons in d+Au collisions at RHIC in the Color Glass Condensate,” *Phys. Rev. Lett.* **105** (2010) 162301, [arXiv:1005.4065 \[hep-ph\]](#).
- [3] F. Dominguez, C. Marquet, B.-W. Xiao, and F. Yuan, “Universality of Unintegrated Gluon Distributions at small  $x$ ,” *Phys. Rev.* **D83** (2011) 105005, [arXiv:1101.0715 \[hep-ph\]](#).
- [4] A. Metz and J. Zhou, “Distribution of linearly polarized gluons inside a large nucleus,” *Phys. Rev. D* **84** (2011) 051503, [arXiv:1105.1991 \[hep-ph\]](#).
- [5] F. Dominguez, J.-W. Qiu, B.-W. Xiao, and F. Yuan, “On the linearly polarized gluon distributions in the color dipole model,” *Phys. Rev. D* **85** (2012) 045003, [arXiv:1109.6293 \[hep-ph\]](#).
- [6] A. Stasto, B.-W. Xiao, and F. Yuan, “Back-to-Back Correlations of Di-hadrons in dAu Collisions at RHIC,” *Phys. Lett.* **B716** (2012) 430–434, [arXiv:1109.1817 \[hep-ph\]](#).
- [7] T. Lappi and H. Mäntysaari, “Forward dihadron correlations in deuteron-gold collisions with the Gaussian approximation of JIMWLK,” *Nucl. Phys.* **A908** (2013) 51–72, [arXiv:1209.2853 \[hep-ph\]](#).
- [8] E. Iancu and J. Laidet, “Gluon splitting in a shockwave,” *Nucl. Phys.* **A916** (2013) 48–78, [arXiv:1305.5926 \[hep-ph\]](#).
- [9] L. Zheng, E. Aschenauer, J. Lee, and B.-W. Xiao, “Probing Gluon Saturation through Dihadron Correlations at an Electron-Ion Collider,” *Phys. Rev. D* **89** (2014) no. 7, 074037, [arXiv:1403.2413 \[hep-ph\]](#).
- [10] T. Altinoluk, N. Armesto, G. Beuf, and A. H. Rezaeian, “Diffractive Dijet Production in Deep Inelastic Scattering and Photon-Hadron Collisions in the Color Glass Condensate,” *Phys. Lett. B* **758** (2016) 373–383, [arXiv:1511.07452 \[hep-ph\]](#).
- [11] Y. Hatta, B.-W. Xiao, and F. Yuan, “Probing the Small- $x$  Gluon Tomography in Correlated Hard Diffractive Dijet Production in Deep Inelastic Scattering,” *Phys. Rev. Lett.* **116** (2016) no. 20, 202301, [arXiv:1601.01585 \[hep-ph\]](#).

- [12] A. Dumitru, T. Lappi, and V. Skokov, “Distribution of Linearly Polarized Gluons and Elliptic Azimuthal Anisotropy in Deep Inelastic Scattering Dijet Production at High Energy,” *Phys. Rev. Lett.* **115** (2015) no. 25, 252301, [arXiv:1508.04438 \[hep-ph\]](#).
- [13] P. Kotko, K. Kutak, C. Marquet, E. Petreska, S. Sapeta, and A. van Hameren, “Improved TMD factorization for forward dijet production in dilute-dense hadronic collisions,” *JHEP* **09** (2015) 106, [arXiv:1503.03421 \[hep-ph\]](#).
- [14] C. Marquet, E. Petreska, and C. Roiesnel, “Transverse-momentum-dependent gluon distributions from JIMWLK evolution,” *JHEP* **10** (2016) 065, [arXiv:1608.02577 \[hep-ph\]](#).
- [15] A. van Hameren, P. Kotko, K. Kutak, C. Marquet, E. Petreska, and S. Sapeta, “Forward di-jet production in p+Pb collisions in the small-x improved TMD factorization framework,” *JHEP* **12** (2016) 034, [arXiv:1607.03121 \[hep-ph\]](#).
- [16] C. Marquet, C. Roiesnel, and P. Taels, “Linearly polarized small- $x$  gluons in forward heavy-quark pair production,” *Phys. Rev. D* **97** (2018) no. 1, 014004, [arXiv:1710.05698 \[hep-ph\]](#).
- [17] J. L. Albacete, G. Giacalone, C. Marquet, and M. Matas, “Forward dihadron back-to-back correlations in  $pA$  collisions,” *Phys. Rev. D* **99** (2019) no. 1, 014002, [arXiv:1805.05711 \[hep-ph\]](#).
- [18] A. Dumitru, V. Skokov, and T. Ullrich, “Measuring the Weizsäcker-Williams distribution of linearly polarized gluons at an electron-ion collider through dijet azimuthal asymmetries,” *Phys. Rev. C* **99** (2019) no. 1, 015204, [arXiv:1809.02615 \[hep-ph\]](#).
- [19] H. Mäntysaari, N. Mueller, and B. Schenke, “Diffractive Dijet Production and Wigner Distributions from the Color Glass Condensate,” *Phys. Rev. D* **99** (2019) no. 7, 074004, [arXiv:1902.05087 \[hep-ph\]](#).
- [20] F. Salazar and B. Schenke, “Diffractive dijet production in impact parameter dependent saturation models,” *Phys. Rev. D* **100** (2019) no. 3, 034007, [arXiv:1905.03763 \[hep-ph\]](#).
- [21] H. Mäntysaari, N. Mueller, F. Salazar, and B. Schenke, “Multigluon Correlations and Evidence of Saturation from Dijet Measurements at an Electron-Ion Collider,” *Phys. Rev. Lett.* **124** (2020) no. 11, 112301, [arXiv:1912.05586 \[nucl-th\]](#).
- [22] R. Boussarie, H. Mäntysaari, F. Salazar, and B. Schenke, “The importance of kinematic twists and genuine saturation effects in dijet production at the Electron-Ion Collider,” *JHEP* **09** (2021) 178, [arXiv:2106.11301 \[hep-ph\]](#).
- [23] P. Kotko, K. Kutak, S. Sapeta, A. M. Stasto, and M. Strikman, “Estimating nonlinear effects in forward dijet production in ultra-peripheral heavy ion collisions at the LHC,” *Eur. Phys. J. C* **77** (2017) no. 5, 353, [arXiv:1702.03063 \[hep-ph\]](#).
- [24] Y. Hagiwara, Y. Hatta, R. Pasechnik, M. Tasevsky, and O. Teryaev, “Accessing the gluon Wigner distribution in ultraperipheral  $pA$  collisions,” *Phys. Rev. D* **96** (2017) no. 3, 034009, [arXiv:1706.01765 \[hep-ph\]](#).
- [25] S. R. Klein and H. Mäntysaari, “Imaging the nucleus with high-energy photons,” *Nature Rev. Phys.* **1** (2019) no. 11, 662–674, [arXiv:1910.10858 \[hep-ex\]](#).
- [26] Y. Hatta, B.-W. Xiao, F. Yuan, and J. Zhou, “Azimuthal angular asymmetry of soft gluon radiation in jet production,” *Phys. Rev. D* **104** (2021) no. 5, 054037, [arXiv:2106.05307 \[hep-ph\]](#).
- [27] E. Iancu and Y. Mulian, “Forward dijets in proton-nucleus collisions at next-to-leading order: the real corrections,” *JHEP* **03** (2021) 005, [arXiv:2009.11930 \[hep-ph\]](#).
- [28] P. Caucal, F. Salazar, and R. Venugopalan, “Dijet impact factor in DIS at next-to-leading order in the Color Glass Condensate,” *JHEP* **11** (2021) 222, [arXiv:2108.06347 \[hep-ph\]](#).
- [29] E. Iancu and R. Venugopalan, “The color glass condensate and high energy scattering in QCD,” [arXiv:hep-ph/0303204](#).
- [30] F. Gelis, E. Iancu, J. Jalilian-Marian, and R. Venugopalan, “The Color Glass Condensate,” *Ann.Rev.Nucl.Part.Sci.* **60** (2010) 463–489, [arXiv:1002.0333 \[hep-ph\]](#).
- [31] Y. V. Kovchegov and E. Levin, *Quantum chromodynamics at high energy*. Cambridge University Press, 2012.
- [32] A. Mueller, B.-W. Xiao, and F. Yuan, “Sudakov double logarithms resummation in hard processes in the small- $x$  saturation formalism,” *Phys. Rev. D* **88** (2013) no. 11, 114010, [arXiv:1308.2993 \[hep-ph\]](#).
- [33] J. Bartels, H. Jung, and M. Wusthoff, “Quark - anti-quark gluon jets in DIS diffractive dissociation,” *Eur. Phys. J. C* **11** (1999) 111–125, [arXiv:hep-ph/9903265](#).
- [34] Y. V. Kovchegov, “Diffractive gluon production in proton nucleus collisions and in DIS,” *Phys. Rev. D* **64** (2001) 114016, [arXiv:hep-ph/0107256](#). [Erratum: *Phys.Rev.D* **68**, 039901 (2003)].
- [35] M. Wusthoff, “Large rapidity gap events in deep inelastic scattering,” *Phys. Rev. D* **56** (1997) 4311–4321, [arXiv:hep-ph/9702201](#).
- [36] K. J. Golec-Biernat and M. Wusthoff, “Saturation in diffractive deep inelastic scattering,” *Phys. Rev. D* **60** (1999) 114023, [arXiv:hep-ph/9903358](#).
- [37] E. Iancu, A. H. Mueller, and D. N. Triantafyllopoulos, *in preparation*.
- [38] A. Accardi *et al.*, “Electron Ion Collider: The Next QCD Frontier: Understanding the glue that binds us all,” *Eur. Phys. J. A* **52** (2016) no. 9, 268, [arXiv:1212.1701 \[nucl-ex\]](#).
- [39] E. Aschenauer, S. Fazio, J. Lee, H. Mantysaari, B. Page, B. Schenke, T. Ullrich, R. Venugopalan, and P. Zurita, “The electron-ion collider: assessing the energy dependence of key measurements,” *Rept. Prog. Phys.* **82** (2019) no. 2, 024301, [arXiv:1708.01527 \[nucl-ex\]](#).
- [40] **LHeC, FCC-he Study Group** Collaboration, P. Agostini *et al.*, “The Large Hadron-Electron Collider at the HL-LHC,” *J. Phys. G* **48** (2021) no. 11, 110501, [arXiv:2007.14491 \[hep-ex\]](#).
- [41] I. Balitsky, “Operator expansion for high-energy scattering,” *Nucl. Phys.* **B463** (1996) 99–160, [arXiv:hep-ph/9509348](#).
- [42] Y. V. Kovchegov, “Small- $x$  F2 structure function of a nucleus including multiple pomeron exchanges,” *Phys. Rev. D* **60** (1999) 034008, [arXiv:hep-ph/9901281](#).
- [43] J. Jalilian-Marian, A. Kovner, A. Leonidov, and H. Weigert, “The BFKL equation from the Wilson renormalization group,” *Nucl. Phys.* **B504** (1997) 415–431, [arXiv:hep-ph/9701284](#).

- [44] J. Jalilian-Marian, A. Kovner, A. Leonidov, and H. Weigert, “The Wilson renormalization group for low  $x$  physics: Towards the high density regime,” *Phys.Rev.* **D59** (1998) 014014, [arXiv:hep-ph/9706377](#) [[hep-ph](#)].
- [45] A. Kovner, J. G. Milhano, and H. Weigert, “Relating different approaches to nonlinear QCD evolution at finite gluon density,” *Phys. Rev.* **D62** (2000) 114005, [arXiv:hep-ph/0004014](#).
- [46] E. Iancu, A. Leonidov, and L. D. McLerran, “Nonlinear gluon evolution in the color glass condensate. I,” *Nucl. Phys.* **A692** (2001) 583–645, [arXiv:hep-ph/0011241](#).
- [47] E. Iancu, A. Leonidov, and L. D. McLerran, “The renormalization group equation for the color glass condensate,” *Phys. Lett.* **B510** (2001) 133–144, [arXiv:hep-ph/0102009](#).
- [48] E. Ferreiro, E. Iancu, A. Leonidov, and L. McLerran, “Nonlinear gluon evolution in the color glass condensate. II,” *Nucl. Phys.* **A703** (2002) 489–538, [arXiv:hep-ph/0109115](#).
- [49] L. D. McLerran and R. Venugopalan, “Computing quark and gluon distribution functions for very large nuclei,” *Phys. Rev.* **D49** (1994) 2233–2241, [arXiv:hep-ph/9309289](#).
- [50] L. D. McLerran and R. Venugopalan, “Green’s functions in the color field of a large nucleus,” *Phys. Rev.* **D50** (1994) 2225–2233, [arXiv:hep-ph/9402335](#).
- [51] E. Levin and M. Wusthoff, “Photon diffractive dissociation in deep inelastic scattering,” *Phys. Rev. D* **50** (1994) 4306–4327.